Lipid recovery from Nannochloropsis gaditana using the wet pathway: Investigation of the operating parameters of bead milling and centrifugal extraction

Vladimir Heredia, Jeremy Pruvost, Olivier Gonçalves, Delphine Drouin, Luc Marchal

▶ **To cite this version:**

Vladimir Heredia, Jeremy Pruvost, Olivier Gonçalves, Delphine Drouin, Luc Marchal. Lipid recovery from Nannochloropsis gaditana using the wet pathway: Investigation of the operating parameters of bead milling and centrifugal extraction. Algal Research - Biomass, Biofuels and Bioproducts, 2021, 56, pp.102318. 10.1016/j.algal.2021.102318 . hal-03246073

HAL Id: hal-03246073
https://hal.inrae.fr/hal-03246073v1

Submitted on 24 May 2023

HAL is a multi-disciplinary open access archive for the deposit and dissemination of scientific research documents, whether they are published or not. The documents may come from teaching and research institutions in France or abroad, or from public or private research centers.

L'archive ouverte pluridisciplinaire **HAL**, est destinée au dépôt et à la diffusion de documents scientifiques de niveau recherche, publiés ou non, émanant des établissements d'enseignement et de recherche français ou étrangers, des laboratoires publics ou privés.

Distributed under a Creative Commons Attribution - NonCommercial 4.0 International License

Version of Record: https://www.sciencedirect.com/science/article/pii/S2211926421001375
Manuscript_ff2dd337b95e048b496b60f832b06b0d

Lipid recovery from *Nannochloropsis gaditana* using the wet pathway: investigation of the operating parameters of bead milling and centrifugal extraction

Vladimir Heredia[a], Jeremy Pruvost[a], Olivier Gonçalves[a], Delphine Drouin[a], Luc Marchal[a,*]

[a] *Université de Nantes, Oniris, GEPEA, UMR 6144 F-44600, Saint-Nazaire, France*

Abstract

The aim of this work is to track and optimize lipid recovery from *Nannochloropsis gaditana* in wet extraction operations. No significant differences in biomass concentration were found when disrupting microalgal suspensions of up to 30 g/L dry weight, but disruption efficiency differed depending on their physiological states. It took 5.8 minutes in a bed milling device to disrupt 80% of the cells in a nitrogen-depleted culture (10-30 g/L), compared to 4.8 minutes for a nitrogen-replete culture (10-30 g/L). The fatty acids released were then recovered by two different methods: one using a centrifugal partition extractor device and the other using a continuous centrifugal extractor device. For the latter, Box-Behnken RSM analysis showed that the interaction between biomass concentration and solvent inlet rate had the greatest influence on lipid recovery. Up to 84% of the triacylglycerol was recovered using 7.9 g/L of algal suspension at 5.4 mL/min, and treated with 8.9 mL/min of 2-methyl-tetra-hydrofuran.

Keywords: Biodiesel, wet extraction, bead milling, centrifugal extraction, experimental design

1. Introduction

Over the last 20 years or so, biofuels from microalgae, such as biodiesel, have been considered as renewable fuels with which to address the energy crisis, and an option with

*Corresponding author
Email address: luc.marchal@univ-nantes.fr (Luc Marchal)

© 2021 published by Elsevier. This manuscript is made available under the CC BY NC user license
https://creativecommons.org/licenses/by-nc/4.0/

regard to mitigating climate change (CO_2 capture)[1]. The biodiesel production process involves the production of fatty acids (FAs) by microalgae (which are stored under stress conditions), the recovery of these energy-rich compounds, and further chemical conversion of them.

There are several microalgae species which can accumulate FAs. The *Nannochloropsis* genus, in particular, is a diverse collection of microalgae comprising 6 species and several sub-strains; most of these have been widely studied for biodiesel production due to their high lipid content under conditions of stress (up to $60\%_X$) [2, 3, 4, 5]. *Nannochloropsis gaditana* is one of the most promising strains, producing high levels of lipids [6]. It is well known that applying stresses such as nitrogen limitation and high light exposure to microalgae triggers the accumulation of FAs, in particular Triacylglycerol molecules (TAG) [6, 7, 8]. Stress also seems to affect cell resistance to disruption. It has been shown that the *Nannochloropsis* genus has a relatively thin cell wall in optimal growing conditions, but when it is exposed to nitrogen limitation the mechanical resistance of the cell is somehow increased [2, 9]. This effect could be linked to changes in the cell size or lipid fraction of the cell wall [10, 11, 12].

Although many technologies have been developed for FAs recovery [13, 14, 1, 15, 16], not all of them can be applied in the biodiesel context, mainly because the processes used are not always as suistainable, energy-efficient or economically viable as expected.

Compared to the energy-intensive operations of the dry pathway, such as biomass drying and solid-liquid extraction, the wet pathway with its technique of cell disruption combined with liquid-liquid extraction is a tested option for developing an energy-efficient process for recovering lipids from microalgae [9, 17, 18, 19, 20]. During cell disruption, many intracellular components, including FAs, are released into the liquid culture and can then be recovered using solvents. This dispenses with the drying or dewatering step involved with the dry pathway and reduces the overall energy required [17, 21, 22, 23].

Cell disruption techniques include biochemical methods (*e.g.* enzymes, chemical treatments, osmotic shock) and mechanical methods (*e.g.* microwaves, ultrasonication, bead milling, high-pressure homogenization, electroporation) [24, 16]. Mechanical methods are advantageous because additional reactive compounds, which may degrade or degenerate beneficial intracellular compounds, are not required. Also, mechanical meth-

ods may be less species-specific than biochemical methods, and for some a wider range of wet biomass concentrations can be treated even for continuous operation. However, these techniques still need improvement in terms of energy consumption and biomass concentration efficiency before they can be used in the wet pathway process for biodiesel, and in terms of understanding and optimizing the undesired effects of some microalgal intracellular compounds on other downstream processes (*e.g.* liquid-liquid extraction by solvents)[24, 9, 25, 26, 16, 23].

Traditional lipid extraction methods by solvents use a mixture of $CHCl_3$ and methanol [27, 28]. Although non-protic or aprotic polar solvents like hexane and $CHCl_3$ [29] have high lipid-extraction yields, their use at industrial scale would exacerbate environmental and health problems [30]. Aprotic solvents like ethyl acetate and 2-methyl-tetra-hydrofuran are an alternative; these are also known as green solvents because they are produced from renewable raw materials. 2-methyl-tetra-hydrofuran, heptane and 8 others have been screened previously for their efficiency in short-time wet extraction. 2-methyl-tetra-hydrofuran in particular minimizes the energy needed for solvent recycling and presents low solubility in water [9].

Liquid-liquid (L-L) extraction is a method widely used for separating a solute from one liquid (*i.e.* microalgal culture feed) into another with a relative preference for the solute (*i.e.* solvent). Efficiency depends mainly on the distribution coefficient of the L-L system (and therefore the choice of solvent), the surface and time of contact between phases (related to mixing), the concentration of the solute (*i.e.* lipid availability) and operating parameters such as temperature and rate of solvent/feed. At industrial scale, these parameters can be modulated in mixers/reactors (batch operation) or mixer-settlers and columns (continuous operation). However, this equipment often requires an additional separation operation (large separatory funnel or industrial centrifugation/decantation). In this regard, an approach employing intensified operations would integrate these technologies and eventually lead to smaller, more energy-efficient process equipment [31, 32].

One way of intensifying wet extraction is to use processes based on centrifugal force, for improved mixing and separation. Systems like continuous centrifugal extraction (CCE) (Fig. 1a) are designed for continuous L-L extraction and simultaneous separation of the phases [33]. CCE mixes two input streams - solvent and algal culture feed

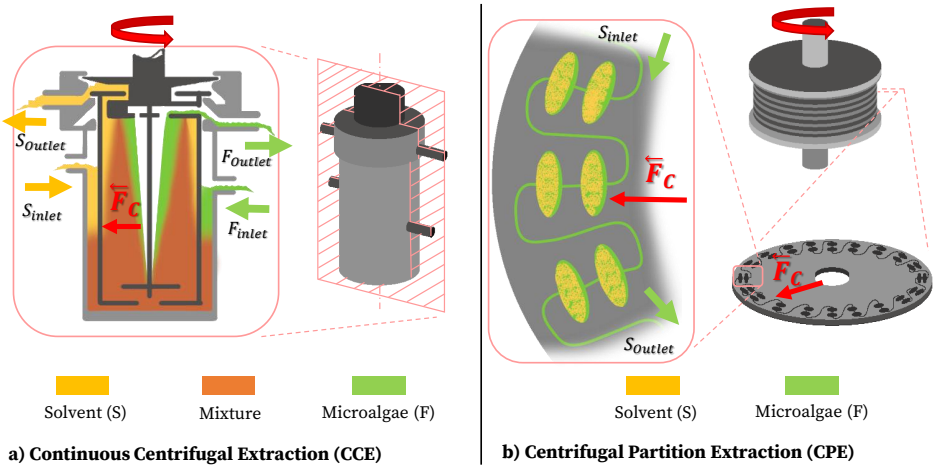

Figure 1: Continuous Centrifugal Extraction and Centrifugal Partition Extraction comparison diagrams. F_C is the centrifugal force vector.

(rich in lipids) - in a common rotary chamber, the speed of which can be modulated. Under the right conditions, two separate outlet flows are recovered during extraction: the raffinate fraction - which is mostly lean culture, and the extract fraction, which is mostly solvent. This equipment is promising for reducing solvent consumption and simplifying scale-up of the wet-extraction process due to its adjustable flow-rate capacity and the ability to connect several modules in series. However, there are no reports on the use of CCE for purely biotechnological applications or biofuel production [34, 32].

Another interesting approach for wet-extraction is to use a centrifugal partition extraction (CPE) device (Fig. 1b). These devices have been widely used for separation and recovery purposes in the biotechnology and nutrition industries [33]. The principle is similar to L-L chromatography but with no solid support to retain the solutes; it is based on the partition coefficient between two non-miscible solvents. CPE devices such as, centrifugal partition chromatography (CPC) have a series of small chambers filled with solvent as a stationary phase. The stationary phase inside is maintained by applying a centrifugal force to the entire series of chambers. A mobile phase is then pumped into the system, enabling interaction with the solvent. This way, the solvent elutes the solutes every time it enters the chambers. With this technology, the amount of solvent used and the operating time are considerably reduced compared to conventional extrac-

tion processes, including CCE [35]. For this reason, CPE is a useful comparison point for efficiency.

Some parameters still need to be adjusted for scaling up centrifugal lipid extraction for biodiesel production. These include: 1) the availability of lipids for the extraction (lipid concentration function and percentage of disrupted biomass); 2) the establishment of an adequate solvent/feed ratio for optimal mass transfer; 3) the absence of emulsion (regularly promoted by the release of intracellular proteins and pH changes after cell disruption).

Analyzing the role of the above parameters in isolation in the extraction process would be inefficient in terms of time, resources and unknown related interactions. One strategy for analyzing and optimizing the multiple factors that interact in the phenomenon is the response surface methodology (RSM). However, prior to running an RSM, a few exploratory experiments are required to ascertain the trends of the variables.

The aim of this work is therefore to enhance lipid recovery from *Nannochloropsis gaditana* by first maximizing lipid availability via bead milling, then optimizing the main parameters using CCE technology. The optimal lipid recovery obtained is then compared with a reference CPE and the resulting operational problems discussed in terms of biodiesel application.

2. Materials and Methods

2.1. Microalgal Cultures

The microalga *Nannochloropsis gaditana* CCMP527 (NCMA, USA) was grown in artificial sea water (ASW) [36] enriched with CONWAY solution as the culture medium. ASW is prepared using (mM): NaCl, 248; Na_2SO_4, 17.1; KCl, 5.49; H_3BO_3, 0.259; NaF, 0.045; $MgCl_2$-$6H_2O$, 32.24; $CaCl_2$-$2H_2O$, 0.626; KBr, 0.497; $SrCl_2$-$6H_2O$, 0.056; $NaHCO_3$, 1.42. CONWAY solution uses $NaNO_3$ as the source of nitrogen, at 10.6 mM. However, for the experiments referred to as N-replete (optimal conditions), the amount of NO_3 was doubled to 21.2 mM to ensure there was no nitrogen limitation. For the cultures referred to as N-depleted (starved conditions), a CONWAY solution was prepared without NO_3, and this was added in the same quantity as for the replete culture. All cultures

were inoculated with a 10% inoculum/medium ratio using a pre-culture in exponential cell growth.

Three photobioreactors (PBRs) were used to supply enough biomass for the work. For the early experiments related to cell disruption optimization and solvent choice, two were set outdoors in France in late summer 2018 (47°15'06.5" N, 2°15'34.5" W) in 170-litre flat-panel airlift PBRs (Subitec, Germany). These reactors were operated in batch mode with the pH regulated at 8 by manual injection of 98% CO2 (gas). For the experiments related to Box-Behnken RSM, a single 170-litre flat-panel airlift PBR (HECtor PBR) was operated indoors in batch mode. A description of the reactor is given by Pruvost et al. [37]. This reactor was irradiated with artificial LED light, simulating the average annual irradiation (photon flux density 269 $\mu mol/m^2 \cdot s$) and solar cycles of the above outdoor conditions. The pH was also set at 8 by automatic CO_2 (gas) injection.

The biomass from the depleted and replete cultures was harvested using a continuous centrifuge (DRA320VX Rousselet Robatel, France) at 6000 rpm (8064 rcf). The sludge (biomass concentration 40 g/L) was then diluted using a phosphate buffer saline (PBS) solution to obtain 1, 5, 10, 20 and 30 g/L for cell disruption optimization, and 2, 5 and 10 g/L for the RSM. Note that in addition to the biomass concentration usually obtained directly from the culture system (1-5 g/L), the range of biomass concentrations in this case was increased to 30 g/L to simulate the possible use of other pre-concentration processes for potential medium recycling (such as dissolved air flotation).

2.2. Dry Weight Analysis

Glass fiber filters with a pore diameter of 0.45 μm (Whatman GF/F) were pre-weighed. 10 mL samples were taken from the PBRs and filtered in triplicate. The filtered biomass was then washed with 3 equal volumes of NH_4HCO_2 1.19 M and 3 equal volumes of MiliQ water to remove culture medium salts. The filters were dried at 103 °C for 1 hour (no further time needed to achieve weight stabilization) and then weighed. The biomass concentration (represented by X) was considered as the weight difference between the dry biomass and the empty filters for each culture volume. The values reported correspond to the mean values in a triplicate dry weight assay.

2.3. Bead Milling

To carry out cell disruption, a continuous bead mill was used in the laboratory (DYNO-Mill KD, Multilab, WAB, Switzerland). The grinding chamber ($\approx$ 0.561 L) connected to an agitator disc (64 mm diameter) was filled to 80% with 0.5 mm diameter glass grinding beads. During the process, milling was carried out at an impeller tip speed of 14 m/s and a flow biomass inlet rate of 9 L/h, with reference to Zinkoné et al. [25].

Three dilutions (10, 20, 30 g/L) for each N-depleted and N-replete outdoor culture were passed through the bead milling device between 1 and 5 times. The corresponding aliquot was analyzed after each time to determine the associated disruption rate.

2.4. Quantification of Cell Disruption

The cells were counted digitally using image analysis and a Malassez cell-counting chamber under microscope. First, a diluted sample was prepared to avoid saturating the number of cells per image, but enough to provide a representative aliquot of the culture [25]. Then a Malassez double chamber was prepared and focused at 40x using an optical microscope connected to a camera (Axio MRC Cam at Axio Scope A1 microscope, Carl Zeiss, Germany). The camera took 40 pictures of each sample, which were then analyzed using image-analysis software (ImageJ v.1.52o, NIH, USA) to distinguish images-like-noise and images-like-cells. The cell surface was calculated in μm^2 for all images-like-cells, based on the distance-to-pixel ratio.

This method identified the cell size, shape and surface distribution of the original culture and compared it to the corresponding values after cell disruption enabling cell debris to be distinguished from undisrupted cells. The cell count and statistical information were then gathered using a MATLAB algorithm (Math-Works, US). Prior to using this method, it was validated with direct microscope counting (data not shown).

The microalgal cell disruption rate τ_D was defined as the complementary fraction of the ratio of cells counted after bead milling to those counted before the process.

2.5. Total Fatty Acid (TFA) and Triacylglycerol (TAG) Extraction Efficiency and Quantification

To measure the TFA content, the organic fractions from extraction experiments were recovered and the corresponding solvent evaporated. The following analysis protocol is

adapted from Moutel et al. [38]. An internal standard solution of a known C17:0 fatty acid concentration and $CHCl_3$/MeOH was added to corroborate the subsequent findings.

To summarize, the sample was derivatized using BF_3 (catalyst) and MeOH at 96°C for 10 minutes (VWR International, US). Following the reaction, the sample was washed using distilled water saturated in hexane to remove catalyst residues. The organic phase was then recovered and measured by gas chromatography using a flame ionization detector (GC–FID, Agilent Technologies, USA). Fatty acid methyl esters (FAMEs) were determined by comparing their retention time with those of the standards ones used for calibration. The concentration of each FAME was calculated with Chemstation software (Agilent Technologies, USA), using C17:0 fatty acid as the internal standard.

TAG content was determined by taking an aliquot of the organic fractions from the extraction experiment and processing it by HPTLC (CAMAG, Switzerland). Samples between 1 and 20 μL were placed on silica gel plates (20 x 10 cm; Merck Group, Germany) by auto-sampler. A self-designed mix of polar and non-polar lipids(Sigma–Aldrich, US) was also placed on the plate as the standard. After sample migration, the plate was revealed in a chromatogram immersion device with a TLC plate heater, using an ortho-phosphoric acid and copper sulphate solution. Data acquisition was by TLC Scanner 3 (VisionCats,CAMAG, Switzerland) and related software.

The results for TFA or TAG per gram of algal biomass treated are shown as $TFA\%_X$ or $TAG\%_X$. The extraction efficiency is represented by:

$$\eta_{E,i} = (i_j)/(i_{CHCl_3/MeOH}) \tag{1}$$

where i is either $TFA\%_X$ or $TAG\%_X$ extraction carried out with a specific solvent, j.

2.6. Choice of Solvent and Standard Extractions

To find out either the TFA or TAG content, $CHCl_3$/Methanol 2:1 v/v (Fisher Sci, US) was used as a reference solvent for extractions. Other solvents used for comparison assays were heptane, Hep (Emsure-Merck, Germany), ethyl acetate, EtoAc (Fisher Sci, US) and 2-methyl-tetra-hydrofuran, Me-THF (Acros Organics-Thermo Fisher Sci, US). Their main properties are summarized in Table 1.

Samples from the depleted cultures were passed through a high-pressure homogenizer (Constant Systems Ltd, UK) three times at 2.7 Kbar and 10 °C. Passing the samples

Table 1: Main physicochemical properties of heptane (Hep), ethyl acetate (EtoAc) and 2-methyl-tetrahydrofuran (Me-THF)

	Hep	**EtoAc**	**Me-THF**
Molecular Formula	C_7H_{16}	$C_4H_8O_2$	$C_5H_{10}O$
Density at 20° C - ρ_S (g/mL)	0.684	0.902	0.854
Vapor pressure at 20° C (mmHg)	34.5	73	102
Boiling temperature at P_{atm} (° C)	98.4	77.1	80.2
Viscosity at 25° C (cP)	0.376	0.423	0.46
Solubility in water at 20° C (wt%)	2.2 (25° C)	8.7	14.1
Reference	[39]	[39]	[40]

through the equipment three times ensured total destruction of the cells, which was verified by microscope observation. The suspension was mixed with the respective solvent at 1:2 v/v (solvent per aqueous phase) for 4 hours at 23 °C, the organic phase was then recovered and the TFA and TAG concentration determined for the solvents tested.

2.7. Continuous Centrifugal Extraction

The extraction system used was a mono-stage continuous centrifugal extraction (CCE) device - type BXP 012 (Rousselet Robatel, France) using N-depleted biomass from the HECtor PBR. Biomass concentration was adjusted to the target values (2,5,10 g/L) and then disrupted in the bead mill to obtain a cell disruption rate τ_D of more than 90% (verified by microscope observation). This suspension was considered as the inlet feed.

The rotation speed of the CCE device was set beforehand at between 2000 and 4000 rpm (107-430 rcf) depending on the experiment run. After approximately 20 seconds, the speed was stable and the solvent and feed inlet rates (S and F) were set at the established flow rate into the system. After an additional 30 - 60 seconds, the extract and raffinate fractions (E and R) began to flow out normally and were recovered at the same inlet flow rate, which also enabled verification of the total flow supplied ($ToT = S + F = E + R$). Around 30 mL from each outlet current (E and R) was then collected and analyzed identically by GC–FID and HPTLC to obtain the TFA/TAG extraction efficiency $\eta_{E,i}$ for the experiment run.

2.8. Experimental Design for Continuous Centrifugal Extraction

A Box-Benhken experiment was designed using the data collected from the bead milling optimization and the more efficient solvent. The CCE variables chosen for Box-Benhken RSM optimization were biomass concentration (after harvesting), solvent inlet rate and feed inlet rate. For detailed information on the design of the Box-Benhken and related data processing, see Appendix A.

All the experiment runs were immediately batched-executed at 25°C within the first 30 minutes of bead milling, to avoid undesirable reactions due to interaction between the medium ions and the cell cytoplasm. Samples from each observation unit were stored at -80°C for determination of further TFA/TAG extraction efficiency ($\eta_{E,i}$).

Where emulsification was unavoidable, samples were still taken but centrifuged at 6000 rpm (4226 rcf) and 4°C for 10 minutes (Hettich, Germany), to separate the phases from the two outlets. The organic phase was then analyzed by the same methods as described above.

Using the data obtained according to the experimental design, the specific solvent consumption Γ_j was calculated as follows:

$$\Gamma_j = (S \cdot \rho_j)/(F \cdot X \cdot \eta_{E,i}) \tag{2}$$

where S is the solvent inlet rate and F the feed inlet rate (both in mL/min); ρ_j is the solvent density in g/mL, X is the biomass concentration in the feed in g/mL and $\eta_{E,i}$ is the extraction efficiency. In this work, Γ_j was only calculated for the optimized condition in the CCE and analysis of the comparison with the CPE.

2.9. Centrifugal Partition Extraction

Centrifugal partition extraction (CPE) was carried out for comparison with the final CCE optimization value. Two liters of N-depleted culture at 5 g/L biomass concentration X were passed through the bead mill several times to obtain a cell disruption rate τ_D of more than 90% (verified by microscope observation). This suspension was treated with CPE.

The CPE device (Model A, Kromaton, France) was fitted with a short column (231 chambers) to carry out TAG extraction with Me-THF. The equipment was set for 1 stage

Table 2: Culture conditions after batch operations. X is biomass concentration, TFA total fatty acid content and TAG triacylglycerol content.

Culture system		**X (g/L)**	**SE (n = 3)**	**TFA content ($\%_X$)**	**TAG content ($\%_X$)**	**Index 480/662 nm**
Outdoor	N-Replete	2.29	2.29	8.7	2.2	0.51
Outdoor	N-Depleted	0.54	0.02	28.1	13.4	1.83
Indoor	N-Depleted	1.52	0.01	32.2	28.6	3.34

at 900 rpm (59 rcf, [41]) in non-continuous mode for a column volume of 270 mL and a solvent volume of 140 mL. The disrupted culture suspension was then passed through the system at 25 mL/min, allowing 5 minutes for the extraction (residence time). The solvent and feed volumes and rates were based on Marchal et al. [42] and Ungureanu et al. [35]. The extracted fraction was recovered and analyzed for TAG content and consequently TAG extraction efficiency ($\eta_{E,TAG}$).

3. Results and Discussion

3.1. Final Culture Conditions

Table 2 shows a summary of the final conditions of the cultures used to produce the biomass. After 11 days, the final biomass concentrations for N-depleted and N-replete outdoor cultures were 0.54 and 2.29 g/L (SE = 0.02 and 2.29; n = 3) respectively, with 28.1$\%_X$ and 8.7$\%_X$ of TFA and 13.4$\%_X$ and 2.2$\%_X$ of TAG respectively. The absorbance 480/662 nm index was measured [43] as a reference to compare stress levels between the PBRs. The N-depleted and N-replete values on the final day were 1.83 and 0.51 respectively, indicating that the carotenoids-to-chlorophyll ratio had a strong influence on the N-depleted culture and confirming cell stress compared to the N-replete culture, as expected.

The indoor PBR culture was ended after 13 days. The final biomass concentration was 1.52 g/L (SE = 0.01; n = 3) with 32.2$\%_X$ TFA and 28.6$\%_X$ TAG. The 480/662 nm index was 3.34 at the end of the culture, which also corroborates the cell stress.

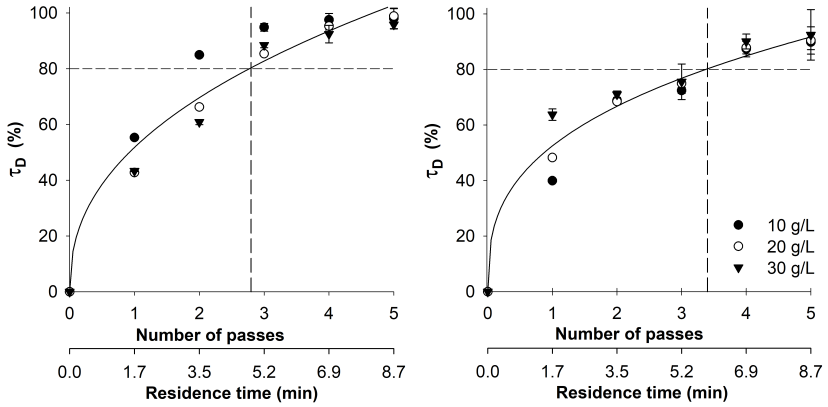

(a) Replete (b) Depleted

Figure 2: Disruption kinetics at bead milling for N-replete and N-depleted cultures. The disruption rate τ_D is plotted for each biomass concentration condition X, and the two-parameter power regression for each physiological state. Error bars for CI (n≈20, $\alpha = 0.05$)

3.2. Cell Disruption Optimization

Fig. 2 plots the cell disruption rate as a function of the physiological state (as a consequence of cells adapting to the culture medium) and biomass concentration, throughout the operating period. Three different biomass concentrations from two different medium conditions (replete and depleted) were processed in a bead mill to find the residence time required (*i.e.* number of passes) to achieve a cell disruption rate of 80%. A one-way analysis of the variance applied to the disruption rate results from the biomass concentration groups at each physiological state revealed that there were no statistically-significant differences between the groups (replete: F(2, 12) = 0.31, p = 0.74 ; depleted: F(2, 12) = 0.22, p = 0.81). Based on this consideration, the whole data set for each physiological state was arranged in a two-parameter power regression, as shown in Fig. 2 ($R^2 = 0.9619$ for replete, $R^2 = 0.9776$ for depleted), and the regression equation enabled calculation of the exact residence time needed for bead milling to disrupt 80% of the cells: 4.8 minutes for replete culture and 5.8 minutes for depleted culture (both for concentrations of between 10 and 30 g/L). The difference is more evident in Fig. 2 where $\tau_D > 80\%$. A minimum of three passes are required for the replete culture (Fig. 2a) and four passes for the depleted culture (Fig. 2b). A comparison of the τ_D from different physiological

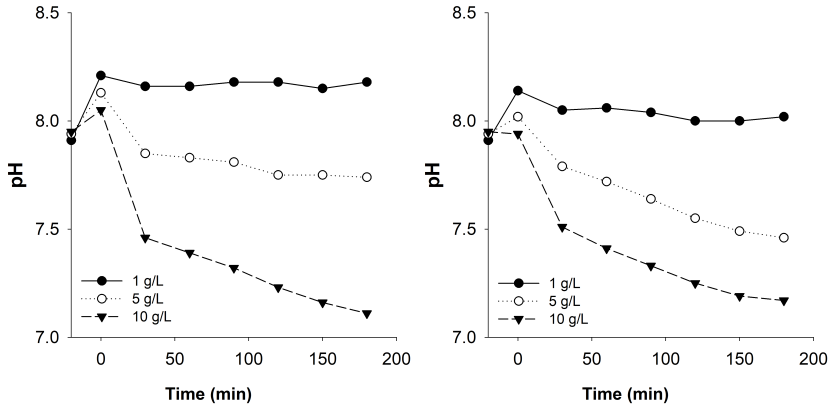

(a) Replete (b) Depleted

Figure 3: pH value of microalga suspension after passing 4 times through a bead mill for N-replete (a) and N-depleted (b) cultures. For each graph, the value on the left represents the pH before milling; the value at zero represents the moment immediately after milling(n = 1).

states shows that *N. gaditana* presents more mechanical resistance to milling when it is harvested in nitrogen-depleted conditions. A similar result using *Nannochloropsis sp.* was obtained by Angles et al. [9].

The final pH value after bead milling is important to preserve the integrity of the molecules to be recovered, and also the workability of the suspension for further steps, mainly emulsification of the lipids and proteins released during the process. For this reason, the pH was monitored for biomass concentrations 1, 5 and 10 g/L and for the two physiological conditions, after cell destruction. The initial pH was 7.9 for each, as shown in Fig. 3. The 10 g/L suspensions for both physiological conditions stabilized the pH almost immediately after disruption (8.2 for replete and 8.0 for depleted). In addition, the 5 g/L suspension of the N-replete culture had a stable and lower pH of 7.8 after 120 minutes. The N-depleted condition at the same concentration and in he same period did not achieve stability (around pH 7.5). The same was observed for the highest suspension concentrations (10 g/L) for both physiological conditions in the 180 minutes test. These conditions tended to attain even lower pH values (around pH 7). This could be explained by the fact that when 5 and 10 g/L cultures are milled, ions like H^+ and other organic compounds are released in proportion to cell concentration and stress level

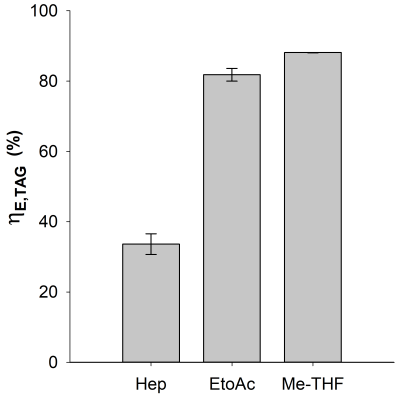

Figure 4: Triacylglycerol extraction efficiency for heptane (Hep), ethyl acetate (EtoAc) and 2-methyl-tetra-hydrofuran (Me-THF). Error bars for SE (n = 2)

(these compounds possibly being accumulated under stress conditions as a cell regulation mechanism [44]). Presumably, the release of these ions and molecules, added to the rest of the culture medium, could interact until the whole solution reaches an equilibrium. The pH stabilization time would depend on the abundance of these molecules and their interaction in the final mixture. It would therefore appear that the suspension needs to be processed for the first 50 minutes after cell disruption, at most, to avoid any undesired interaction, which could affect the recovery process.

3.3. Choice of Solvent for Extraction

Fig. 4 shows the extraction efficiency results for N-depleted biomass using the three solvents tested. Me-THF and EtoAc showed a similar extraction efficiency $\eta_{E,TAG}$: up to 88% and 82% respectively. Heptane had the lowest at 34%. In all cases, TAG represented 89% of the measured TFA, showing that the solvents used have no relevant selectivity for TAG.

In addition, by using cell destruction prior to extraction, the solvents (or mixtures) did not depend on their ability to draw lipids from the cell (such as 2:1 v/v $CHCl_3$/MeOH [28]) but only on their affinity with lipid molecules, since TAG molecules were already released into the medium. This enabled maximization of extraction efficiency and thereby reduction of the amount of solvent used, which would also significantly reduce the investment in solvent required for the whole wet extraction process.

As a result, Me-THF will be selected for future experiments as the best of the three solvents for recovering TAG.

3.4. Centrifugal Partition Extraction

Centrifugal partition extraction (CPE) was used only as a reference to compare the specific solvent consumption (Γ_{Me-THF}) of the optimal CCE results from the Box-Benhken RSM.

For a single TAG extraction carried out with a CPE device, it was possible to treat 2 L at a biomass concentration 5 g/L with only 140 mL of solvent.

These values represent a TAG extraction efficiency $\eta_{\mathrm{E,TAG}}$ of 83% (SE = 3%, n = 3), which corresponds to a specific solvent consumption of Γ_{Me-THF} of 27.7 $g_{\mathrm{Me\text{-}THF}}/g_{\mathrm{TAG}}$.

3.5. Continuous Centrifugal Extraction

The Box-Benhken RSM was chosen as the method for optimizing the main CCE parameters. The optimal value obtained with this method, added to the bead milling results, was expected to provide relevant information on the overall efficiency of the wet-extraction method in the biodiesel context.

Pre-tests were run prior to the main analysis to clarify the operating CCE work zone. Emulsions were readily obtained when the rotation speed of the CCE device exceeded certain limits. These limits varied for each observation unit (OU) but were within the 5000 to 6000 rpm range (670 - 966 rcf). A relationship was observed between this rotational speed limit and the total supplied flow (ToT) for the different substances. Higher speeds promoted separation of the phases, but also the formation of emulsion. This phenomenon could be due to Taylor vortexes occurring during the centrifugal extraction and driving more complex variations in fluid dynamics when the rotation speed was increased [45, 46]. There is therefore a compromise between emulsification and separation when using a CCE module.

Another factor that could influence emulsification and therefore extraction efficiency ($\eta_{E,i}$) is the release of intracellular material into the medium. It has been shown that some microalgae proteins have emulsifying properties [47]. Similarly, the cell debris could also form particle-stabilized emulsions known as Pickering emulsions [48]. Biomass concentration and disruption rate, therefore, also influence this phenomenon; for a given

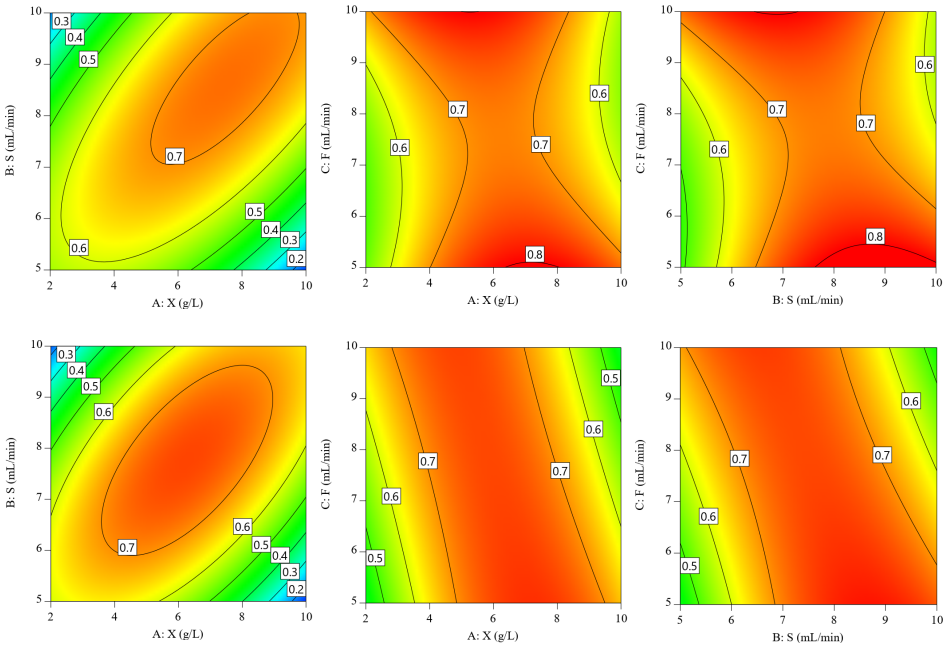

Figure 5: Contour graphs for each interaction between sources for the regression model obtained by Box-Behnken for extraction efficiency, $\eta_{E,i}$ response. The contour lines represent extraction efficiency, $\eta_{E,i}$ levels; a), b) and c) for Total Fatty Acid (TFA) and d), e) and f) for Triacylglycerol (TAG).

high biomass suspension, increasing the disruption rate τ_D will also release emulsifying molecules/particles. Accordingly, additional pre-tests were run to clarify the biomass concentration range to avoid emulsification as far as possible. Normally, cultures above 10 g/L are unmanageable for extraction due to the immediate appearance of an emulsion, even when working at low S/F ratios or low rotation speeds ($<$ 4000 rpm / 429 rcf). For example, when working with suspensions above 10 g/L of biomass, emulsions appeared from 3500 rpm (329 rcf). A higher rotation speed was therefore required for recovering the same outlet flow rates (since $ToT = S + F = E + R$), although no solvent was recovered, just an enhanced emulsion. These pre-tests defined the operational range of biomass concentration as between 2-10 g/L for RSM analysis. Protein content and operational pH were not considered as variables for RSM.

The RSM experimental results are detailed in Appendix A, Table A.3. The resulting contour graphics (Fig. 5) describing the extraction efficiency as a response of the oper-

ational variables may therefore be useful for navigating within the limits of the CCE. Using the biomass - solvent interaction (X - S), as a first reference, Figs. 5a and 5d show the maximal extraction efficiency $\eta_{E,i}$ as being within S: 7-10 mL/min and X: 5-10 g/L. This zone can therefore be transposed to the X-F and S-F interactions (Figs. 5b, 5c, 5e, 5f) where higher efficiencies are found at a low feed rate.

The numerical results obtained (see Appendix A) provide a tool for locating the optimal point for the three simultaneous sources. It was found that $\eta_{\mathrm{E,TFA}} = 0.93$ at $X = 8.3$ g/L, $S = 9.2$ mL/min, $F = 5.0$ mL/min and $\eta_{\mathrm{E,TAG}} = 0.84$ at $X = 7.9$ g/L, $S = 8.9$ mL/min and, $F = 5.4$ mL/min. Both efficiency points were consistent with the previous analyses. The values obtained were higher than with the $CHCl_3$/methanol wet extraction (extraction efficiency, $\eta_{E,i} = 50\%$) carried out by Angles et al. [9]. Remember, however, that the values correspond to the 80% of lipids released in the bead milling operation.

With the optimal point obtained by the experiment design, the specific solvent consumption for CCE was determined as $\Gamma_{Me-THF} = 213.8$ $g_{\mathrm{Me\text{-}THF}}/g_{\mathrm{TAG}}$.

Note that Γ_{Me-THF} is linked to the energy consumption for the whole biodiesel process, since more energy is required for distilling each gram of solvent used to produce each liter of biodiesel. These values show that if scaled up, CPE technology could save 7.8 times more solvent than CCE, even though the two technologies have similar extraction efficiencies.

However, the results for CCE could be improved. On the one hand, this work has demonstrated the relationship between stress levels, biomass concentration and the release of intracellular material with the formation of emulsion, and has revealed the work zone to be avoided when carrying out CCE. In this regard, more research on the optimization of hydrodynamics in the CCE chamber could enable working with higher biomass concentrations, which would increase recovery. On the other hand, CCE efficiency can also be improved by using several devices connected in series (the present work relating to a single module). This approach is also valuable in terms of the scalability of the operation, which is one of the biggest advantages of CCE over CPE.

As stated, many factors other than those relating to the appearance of emulsification (such as pH and temperature) that were not studied in detail in the present work, interact during centrifugal extraction and should be investigated for future experiments in

biodiesel production.

The optimal wet extraction yield of 73% obtained with bead milling combined with CCE (using Me-THF) has been demonstrated as a high-performance TAG recovery technique with the advantage of scalability for the biodiesel process. The process may perform better than extraction yields in the literature. For example, different solvent mixtures and cell disruptions for *N. gaditana* were tested by Ryckebosch et al. [49], where solvents such as hexane/isopropanol, ethyl acetate/hexane and ethanol were found to be the best of six, with extraction yields of 58%, 46% and 52% respectively. Similarly, Sati et al. [50] reviewed extraction yields from other pre-extraction treatments such as mechanical (35%), surfactant (78%) and enzymatic lysis (73%). There are other techniques effective for biodiesel application too, such as the simultaneous distillation and extraction process, which gave a 24% extraction yield with *N. oculata* [51], and microwave combined with super-critical CO_2 extraction, which achieved a 30% extraction yield with *N. salina* [52].

4. Conclusion

Wet extraction operations (bead milling combined with centrifugal extraction) achieved a final TAG recovery of 73% using CCE technology with *Nannochloropsis gaditana* cultivated in N-depleted media. Physiological variables such as cell fragility, and process operating conditions such as harvesting concentration, were found to affect the whole process. The key variables and their interactions during lipid recovery were determined and optimized by RSM analysis. However, CCE uses around eight times more solvent than CPE. Consequently, further intensification of the extraction step is required to combine scalability (*i.e.* the CCE process) with a reduction in solvent consumption and emulsification issues for biodiesel production.

Acknowledgements

VH acknowledges the National Science and Technology Council (CONACyT, Mexico) for his research fellowship. All the authors acknowledge the contributions made by B. Le Gouic, J. Tallec, S. Chollet, L. Herve and M. Cueff

Funding: This research did not receive any specific grant from funding agencies in the public, commercial, or not-for-profit sectors.

CRediT authorship contribution statement

Vladimir Heredia: Conceptualization, Formal analysis, Investigation,Writing - Original Draft. Jeremy Pruvost: Writing - Review & Editing, Supervision. Olivier Gonçalves: Writing - Review & Editing. Luc Marchal: Conceptualization, Investigation, Writing - Review & Editing, Supervision.

Informed Consent, Human/Animal Rights Statement

No conflicts, informed consent, or human or animal rights are applicable to this study.

References

[1] Y. Chisti, Biodiesel from microalgae, Biotechnology Advances 25 (2007) 294–306.

[2] T. A. Beacham, C. Bradley, D. A. White, P. Bond, S. T. Ali, Lipid productivity and cell wall ultrastructure of six strains of Nannochloropsis: Implications for biofuel production and downstream processing, Algal Research 6 (2014) 64–69.

[3] X. Ma, J. Liu, B. Liu, T. Chen, B. Yang, F. Chen, Physiological and biochemical changes reveal stress-associated photosynthetic carbon partitioning into triacylglycerol in the oleaginous marine alga Nannochloropsis oculata, Algal Research 16 (2016) 28–35.

[4] Y. Ma, Z. Wang, C. Yu, Y. Yin, G. Zhou, Evaluation of the potential of 9 Nannochloropsis strains for biodiesel production, Bioresource Technology 167 (2014) 503–509.

[5] D. Bouillaud, V. Heredia, T. Castaing-Cordier, D. Drouin, B. Charrier, O. Gonçalves, J. Farjon, P. Giraudeau, Benchtop flow NMR spectroscopy as an online device for the in vivo monitoring of lipid accumulation in microalgae, Algal Research 43 (2019) 101624.

[6] A. Taleb, J. Pruvost, J. Legrand, H. Marec, B. Le-Gouic, B. Mirabella, B. Legeret, S. Bouvet, G. Peltier, Y. Li-Beisson, S. Taha, H. Takache, Development and validation of a screening procedure of microalgae for biodiesel production: Application to the genus of marine microalgae Nannochloropsis, Bioresource Technology 177 (2015) 224–232.

[7] K. J. Flynn, K. Davidson, A. Cunningham, Relations between carbon and nitrogen during growth of Nannochloropsis oculata (Droop) Hibberd under continuous illumination, New Phytologist 125 (1993) 717–722.

[8] J. Camacho-Rodríguez, A. M. González-Céspedes, M. C. Cerón-García, J. M. Fernández-Sevilla, F. G. Acién-Fernández, E. Molina-Grima, A quantitative study of eicosapentaenoic acid (EPA) production by Nannochloropsis gaditana for aquaculture as a function of dilution rate, temperature and average irradiance, Applied Microbiology and Biotechnology 98 (2014) 2429–2440.

[9] E. Angles, P. Jaouen, J. Pruvost, L. Marchal, Wet lipid extraction from the microalga Nannochloropsis sp.: Disruption, physiological effects and solvent screening, Algal Research 21 (2017) 27–34.

[10] J. H. Janssen, P. P. Lamers, R. C. de Vos, R. H. Wijffels, M. J. Barbosa, Translocation and de novo synthesis of eicosapentaenoic acid (EPA) during nitrogen starvation in Nannochloropsis gaditana, Algal Research 37 (2019) 138–144.

[11] V. Montalescot, T. Rinaldi, R. Touchard, S. Jubeau, M. Frappart, P. Jaouen, P. Bourseau, L. Marchal, Optimization of bead milling parameters for the cell disruption of microalgae: Process modeling and application to Porphyridium cruentum and Nannochloropsis oculata, Bioresource Technology 196 (2015) 339–346.

[12] M. J. Scholz, T. L. Weiss, R. E. Jinkerson, J. Jing, R. Roth, U. Goodenough, M. C. Posewitz, H. G. Gerken, Ultrastructure and composition of the Nannochloropsis gaditana cell wall, Eukaryotic Cell 13 (2014) 1450–1464.

[13] X. B. Tan, M. K. Lam, Y. Uemura, J. W. Lim, C. Y. Wong, K. T. Lee, Cultivation of microalgae

for biodiesel production: A review on upstream and downstream processing, Chinese Journal of Chemical Engineering 26 (2018) 17–30.

[14] M. Axelsson, F. Gentili, A single-step method for rapid extraction of total lipids from green microalgae, PLoS ONE 9 (2014) 17–20.

[15] S. A. Scott, M. P. Davey, J. S. Dennis, I. Horst, C. J. Howe, D. J. Lea-Smith, A. G. Smith, Biodiesel from algae: Challenges and prospects, Current Opinion in Biotechnology 21 (2010) 277–286.

[16] R. Halim, R. Harun, M. K. Danquah, P. A. Webley, Microalgal cell disruption for biofuel development, Applied Energy 91 (2012) 116–121.

[17] H. Taher, S. Al-Zuhair, A. H. Al-Marzouqi, Y. Haik, M. Farid, Effective extraction of microalgae lipids from wet biomass for biodiesel production, Biomass and Bioenergy 66 (2014) 159–167.

[18] T. Dong, E. P. Knoshaug, P. T. Pienkos, L. M. Laurens, Lipid recovery from wet oleaginous microbial biomass for biofuel production: A critical review, Applied Energy 177 (2016) 879–895.

[19] A. K. Lee, D. M. Lewis, P. J. Ashman, Disruption of microalgal cells for the extraction of lipids for biofuels: Processes and specific energy requirements, Biomass and Bioenergy 46 (2012) 89–101.

[20] F. Ghasemi Naghdi, L. M. González González, W. Chan, P. M. Schenk, Progress on lipid extraction from wet algal biomass for biodiesel production, Microbial Biotechnology 9 (2016) 718–726.

[21] R. Halim, B. Gladman, M. K. Danquah, P. A. Webley, Oil extraction from microalgae for biodiesel production, Bioresource Technology 102 (2011) 178–185.

[22] H. M. Amaro, A. C. Guedes, F. X. Malcata, Advances and perspectives in using microalgae to produce biodiesel, Applied Energy 88 (2011) 3402–3410.

[23] J. Y. Lee, C. Yoo, S. Y. Jun, C. Y. Ahn, H. M. Oh, Comparison of several methods for effective lipid extraction from microalgae, Bioresource Technology 101 (2010) S75–S77.

[24] J. Kim, G. Yoo, H. Lee, J. Lim, K. Kim, C. W. Kim, M. S. Park, J. W. Yang, Methods of downstream processing for the production of biodiesel from microalgae, Biotechnology Advances 31 (2013) 862–876.

[25] T. R. Zinkoné, I. Gifuni, L. Lavenant, J. Pruvost, L. Marchal, Bead milling disruption kinetics of microalgae: Process modeling, optimization and application to biomolecules recovery from Chlorella sorokiniana, Bioresource Technology 267 (2018) 458–465.

[26] C. Safi, C. Frances, A. V. Ursu, C. Laroche, C. Pouzet, C. Vaca-Garcia, P. Y. Pontalier, Understanding the effect of cell disruption methods on the diffusion of chlorella vulgaris proteins and pigments in the aqueous phase, Algal Research 8 (2015) 61–68.

[27] J. Folch, M. Lees, G. Sloane Stanley, A simple method for the isolation and purification of total lipides from animal tissues 55 (1987) 999–1033.

[28] E. G. Bligh, W. J. Dyer, A Rapid Method Of Total Lipid Extraction And Purification, Canadian Journal of Biochemistry and Physiology 37 (1959) 911–917.

[29] P. Li, K. Sakuragi, H. Makino, Extraction techniques in sustainable biofuel production: A concise review, Fuel Processing Technology 193 (2019) 295–303.

[30] P. Watts, Chloroform, Technical Report 58, World Health Organization, Geneva, Switzerland, 2004. URL: `https://www.who.int/ipcs/publications/cicad/en/`.

[31] D. Reay, C. Ramshaw, A. Harvey (Eds.), Process Intensification, Elsevier, 2008. doi:10.1016/B978-0-7506-8941-0.X0001-6.

[32] B. Seyfang, A. Klein, T. Grützner, Extraction Centrifuges—Intensified Equipment Facilitating Modular and Flexible Plant Concepts, ChemEngineering 3 (2019) 17.

[33] M. Bojczuk, D. Żyżelewicz, P. Hodurek, Centrifugal partition chromatography – A review of recent applications and some classic references, Journal of Separation Science 40 (2017) 1597–1609.

[34] K. Schügerl, Solvent Extraction in Biotechnology, volume 8, Springer Berlin Heidelberg, Berlin, Heidelberg, 1994. doi:10.1007/978-3-662-03064-6.

[35] C. Ungureanu, L. Marchal, A. A. Chirvase, A. Foucault, Centrifugal partition extraction, a new method for direct metabolites recovery from culture broth: Case study of torularhodin recovery from Rhodotorula rubra, Bioresource Technology 132 (2013) 406–409.

[36] J. A. Berges, D. J. Franklin, P. J. Harrison, Evolution of an artificial seawater medium: Improvements in enriched seawater, artificial water over the last two decades, Journal of Phycology 37 (2001) 1138–1145.

[37] J. Pruvost, G. Van Vooren, B. Le Gouic, A. Couzinet-Mossion, J. Legrand, Systematic investigation of biomass and lipid productivity by microalgae in photobioreactors for biodiesel application, Bioresource Technology 102 (2011) 150–158.

[38] B. Moutel, O. Gonçalves, F. Le Grand, M. Long, P. Soudant, J. Legrand, D. Grizeau, J. Pruvost, Development of a screening procedure for the characterization of Botryococcus braunii strains for biofuel application, Process Biochemistry 51 (2016) 1855–1865.

[39] S. Kim, J. Chen, T. Cheng, A. Gindulyte, J. He, S. He, Q. Li, B. A. Shoemaker, P. A. Thiessen, B. Yu, L. Zaslavsky, J. Zhang, E. E. Bolton, PubChem 2019 update: improved access to chemical data, Nucleic Acids Research 47 (2019) D1102–D1109.

[40] A.-G. Sicaire, M. A. Vian, A. Filly, Y. Li, A. Bily, F. Chemat, 2-Methyltetrahydrofuran: Main Properties, Production Processes, and Application in Extraction of Natural Products, 2014, pp. 253–268. doi:10.1007/978-3-662-43628-8_12.

[41] L. Marchal, J. Legrand, A. Foucault, Mass transport and flow regimes in centrifuga partition chromatography, AIChE Journal 48 (2002) 1692–1704.

[42] L. Marchal, M. Mojaat-Guemir, A. Foucault, J. Pruvost, Centrifugal partition extraction of β-carotene from Dunaliella salina for efficient and biocompatible recovery of metabolites, Bioresource Technology 134 (2013) 396–400.

[43] M. R. Heath, K. Richardson, T. Kirboe, Optical assessment of phytoplankton nutrient depletion, Journal of Plankton Research 12 (1990) 381–396.

[44] M. A. Borowitzka, The 'stress' concept in microalgal biology—homeostasis, acclimation and adaptation, Journal of Applied Phycology 30 (2018) 2815–2825.

[45] J. T. Stuart, Taylor-Vortex Flow: A Dynamical System, SIAM Review 28 (1986) 315–342.

[46] M. Nakase, K. Takeshita, Numerical and Experimental Study on Oil-water Dispersion in New Countercurrent Centrifugal Extractor, Procedia Chemistry 7 (2012) 288–294.

[47] S. Ebert, L. Grossmann, J. Hinrichs, J. Weiss, Emulsifying properties of water-soluble proteins

543 extracted from the microalgae: Chlorella sorokiniana and Phaeodactylum tricornutum, Food and
544 Function 10 (2019) 754–764.
545 [48] H. Jiang, Y. Sheng, T. Ngai, Pickering emulsions: Versatility of colloidal particles and recent
546 applications, Current Opinion in Colloid & Interface Science 49 (2020) 1–15.
547 [49] E. Ryckebosch, S. P. C. Bermúdez, R. Termote-Verhalle, C. Bruneel, K. Muylaert, R. Parra-
548 Saldivar, I. Foubert, Influence of extraction solvent system on the extractability of lipid components
549 from the biomass of Nannochloropsis gaditana, Journal of Applied Phycology 26 (2014) 1501–1510.
550 [50] H. Sati, M. Mitra, S. Mishra, P. Baredar, Microalgal lipid extraction strategies for biodiesel pro-
551 duction: A review, Algal Research 38 (2019) 101413.
552 [51] C. Dejoye Tanzi, M. Abert Vian, F. Chemat, New procedure for extraction of algal lipids from wet
553 biomass: A green clean and scalable process, Bioresource Technology 134 (2013) 271–275.
554 [52] P. D. Patil, K. P. R. Dandamudi, J. Wang, Q. Deng, S. Deng, Extraction of bio-oils from algae
555 with supercritical carbon dioxide and co-solvents, Journal of Supercritical Fluids 135 (2018) 60–68.
556 [53] G. E. P. Box, D. W. Behnken, Some New Three Level Designs for the Study of Quantitative
557 Variables, Technometrics 2 (1960) 455.
558 [54] S. L. Ferreira, R. E. Bruns, H. S. Ferreira, G. D. Matos, J. M. David, G. C. Brandão, E. G. da Silva,
559 L. A. Portugal, P. S. dos Reis, A. S. Souza, W. N. dos Santos, Box-Behnken design: An alternative
560 for the optimization of analytical methods, Analytica Chimica Acta 597 (2007) 179–186.

Appendix A. CCE operating parameter optimization: RSM approach

A.1. Introduction

The Box-Behnken response surface methodology (RSM) was designed [53, 54] to clarify the interaction between operating parameters in the CCE wet extractor. Contrary to the usual factorial RSM (where variables are arranged in an n-dimensional space and all combinations are considered for the experiment setup), the Box-Behnken RSM is arranged as a spherical set of variables, which means that the number of experiment runs is reduced and the extreme interaction vertices are not considered. It is advantageous because certain combinations of factors (in this work and others) could be physically restrictive or expensive to operate.

Using this RSM, a response surface is obtained that can be modeled and analyzed using the ANOVA method, which looks for the greatest interaction impacting the response.

A.2. experiment setup

The Box-Benhken RSM included 15 observation units (OUs) for three independent factors and one response variable: 12 OUs derived from independent variables around 3 other OUs as replicates of the central point. Ranges and variables were biomass concentration (from bead milling) X = 2, 5, 10 g/L and solvent and feed inlets S and F = 5, 7.5, 10 mL/min each. The results of experiments carried out with all the observations units performed are presented in Table A.3.

The TFA/TAG extraction efficiency ($\eta_{E,i}$) results from the 15 OUs were processed using Design Expert V11 (Stat-Ease, US). For some analyses, the variables were coded as follows: X as A, S as B and F as C. The software provided random experimental design, statistical analysis and numerical and graphical optimization.

A.3. RSM data analysis

After running the Design Expert software, the data were found to fit well with a quadratic-order model. Fig. A.1 shows that with the experiment extraction efficiency $\eta_{E,i}$, which corresponds with a high biomass concentration, X and S cannot actually be fitted into a model because of the sudden increase (mainly due to the unexpected appearance of emulsion at these values).

Table A.3: Experimental results obtained by the Box-Benhken RSM analysis for the Total Fatty Acid ($\eta_{E,TFA}$) and Triacylglycerol ($\eta_{E,TAG}$) extraction efficiencies. OU - observation unit; A, B and C are the coded values for biomass concentration (X), solvent inlet rate (S) and feed inlet rate (F) respectively.

O.U.	**A : X (g/L)**	**B : S (mL/min)**	**C : F (mL/min)**	$\eta_{E,TFA}$	$\eta_{E,TAG}$
1	2,0	7,5	10,0	84%	81%
2	2,0	7,5	5,0	55%	48%
3	2,0	5,0	7,5	42%	41%
4	2,0	10,0	7,5	15%	13%
5	5,0	10,0	5,0	73%	62%
6	5,0	7,5	7,5	70%	74%
7	5,0	7,5	7,5	70%	74%
8	5,0	10,0	10,0	44%	30%
9	5,0	5,0	10,0	78%	79%
10	5,0	5,0	5,0	59%	56%
11	5,0	7,5	7,5	70%	73%
12	10,0	10,0	7,5	82%	80%
13	10,0	7,5	10,0	51%	34%
14	10,0	7,5	5,0	60%	52%
15	10,0	5,0	7,5	21%	19%

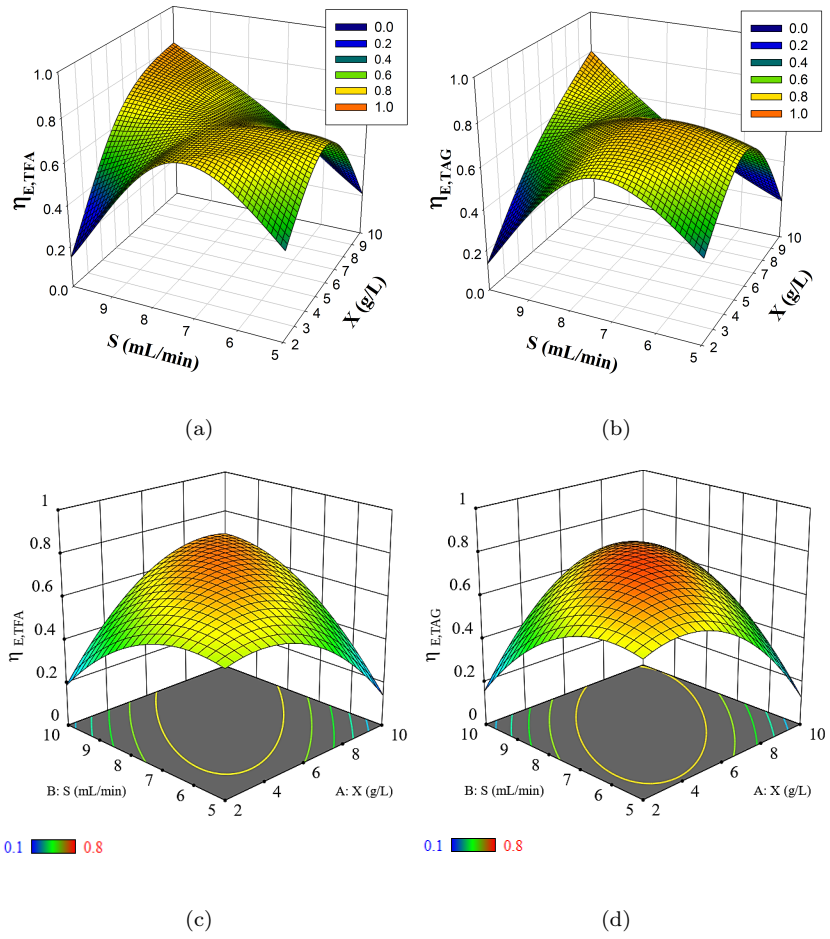

Figure A.1: Raw experiment data and quadratic 3D mesh model for the influence of solvent-to-biomass concentration on extraction efficiency, $\eta_{E,i}$. a) and b) unprocessed data for Total Fatty Acid (TFA) and Triacylglycerol (TAG) respectively. c) and d) data obtained after modeling

Table A.4: Analysis of variance (ANOVA) for modeling of a quadratic order. Values for surface response on Total Fatty Acid (TFA) and Triacylglycerol (TAG) extraction efficiency are shown.

	AGT					TAG				
Source	**SS**	**df**	**Mean Square**	**F-value**	**p-value**	**SS**	**df**	**Mean Square**	**F-value**	**p-value**
Model	0.4980	9	0.0553	2.730	0.141	0.5790	9	0.0643	2.150	0.207
A-Biomass conc.	0.0033	1	0.0033	0.164	0.702	0.0001	1	0.0001	0.003	0.962
B-Solvant	0.0156	1	0.0156	0.770	0.420	0.0026	1	0.0026	0.088	0.779
C-Feed	0.0001	1	0.0001	0.001	0.977	0.0003	1	0.0003	0.010	0.925
AB	0.2179	1	0.2179	10.740	0.022	0.2303	1	0.2303	7.700	0.039
AC	0.0279	1	0.0279	1.380	0.294	0.0557	1	0.0557	1.860	0.231
BC	0.0553	1	0.0553	2.730	0.160	0.0727	1	0.0727	2.430	0.180
A^2	0.0892	1	0.0892	4.400	0.090	0.1307	1	0.1307	4.370	0.091
B^2	0.0765	1	0.0765	3.770	0.110	0.1006	1	0.1006	3.360	0.126
C^2	0.0246	1	0.0246	1.210	0.321	0.0002	1	0.0002	0.007	0.937
Std.Dev.			0.142					0.173		
Mean			0.582					0.546		
C.V.%			24.482					31.700		
R^2			0.831					0.795		

The analysis of variance (Table A.4) showed that first-order sources (A, B and C) seem to have less significance than second-order sources (AB, AC, BC, A^2, B^2 and C^2). On the whole, interactions and additives affected the model response more than isolated variables: AB and A^2 are the only ones below $\alpha = 0.1$. The same trends were obtained for TFA and TAG.

The results reported in the section 3.5 for maximum extraction efficiency in the model were obtained using $\alpha = 0.05$ in the numerical solution provided by the Design Expert software.

The estimated coefficients are shown in table A.5. These represent the expected shift in response per unit factor value, with the other factors constant. To obtain these coefficients using the Box-Benhken RSM, the source values had to be coded as +1 for the higher levels and -1 for the lower ones. This type of analysis enabled identification of the relative impact of the factors by comparing their coefficients. The equation produced with these coefficients could be used to predict the effects in the response, but only within the coded limits of each source.

By ignoring the additive variables, for example, the source AB ($Coeff_{TFA}$: 0.230, $Coeff_{TAG}$: 0.236) was shown to have the greatest proportional effect on extraction effi-

Table A.5: Estimated regression coefficients in terms of coded factors and final equation coefficients in terms of actual factors, both obtained from the quadratic model obtained for Total Fatty Acid (TFA) and Triacylglycerol (TAG) wet-extraction efficiency.

Factor	TFA		TAG	
	Coefficient estimate	**Final equation coefficient**	**Coefficient estimate**	**Final equation coefficient**
Intercept	0.712	-0.792	0.753	-1.973
A- Biomass conc.	0.020	0.0206	0.003	0.0634
B-Solvant	0.045	0.3667	0.018	0.4235
C-Feed	0.002	-0.005	-0.006	0.247
AB	0.230	0.023	0.236	0.0236
AC	-0.082	-0.008	-0.116	-0.012
BC	-0.118	-0.019	-0.135	-0.022
A^2	-0.168	-0.011	-0.204	-0.013
B^2	-0.144	-0.023	-0.165	-0.026
C^2	0.082	0.0131	-0.008	-0.001

ciency $\eta_{E,i}$, followed by an inverse-proportional effect on the relationship between S and F ($\text{Coeff}_{\text{TFA}}$: -0.118, $\text{Coeff}_{\text{TAG}}$: -0.135). This simply means that if more lipids are to be recovered, a higher S should also be used, but the effect is diminished if F is increased in relation to S. A high concentration would require more time and interface contact with the solvent, which can be achieved by reducing the feed rate for CCE. On the other hand, the effect of the additive variables is also highest for A^2 and B^2. Table A.5 also shows the coefficients for the equation in terms of actual factors. This could be used to predict the extraction efficiency $\eta_{E,i}$ for given levels of each factor. Here, the levels should be specified in the original units for each factor.

Nevertheless, neither type of coefficient obtained for regression in this work can be used to accurately predict extraction efficiency $\eta_{E,i}$ precisely, due to the low R^2 and moderate p-value of the model itself. However, R^2 (0.831 for TFA and 0.795 for TAG) indicates only a reasonable correlation between the experimental and predicted values of the response. Despite this, the model still provides important information on the relationship between the parameters, which is clearer when the contour graphs are analyzed.

Note that the reason for using Box-Behnken RSM for this work was to determine the general extraction trend as a function of the main operating parameters (such as biomass concentration and solvent and biomass flow rates) and also to determine an operational CCE work-zone.